Journal of Power Sources 247 (2014) 712–720

Contents lists available at ScienceDirect

Journal of Power Sources

journal homepage: www.elsevier.com/locate/jpowsour

Effect of heat treatment on the activity and stability of carbon supported PtMo alloy electrocatalysts for hydrogen oxidation in proton exchange membrane fuel cells

Ayaz Hassan [a], Alejo Carreras [b], Jorge Trincavelli [b], Edson Antonio Ticianelli [a, *]

[a] Instituto de Quimica de São Carlos, Universidade de São Paulo, Caixa Postal 7 80, São Carlos, SP CEP 13560-970, Brazil
[b] Instituto de Física Enrique Gaviola (IFEG)-CONICET, Facultad de Matemática, Astronomía y Física, Universidad Nacional de Córdoba, Medina Allende s/n, 5016 Córdoba, Argentina

HIGHLIGHTS

- The CO tolerance and stability of heat-treated carbon supported PtMo (60:40 at.%) catalysts are investigated.
- The PtMo/C catalyst treated at 600 °C shows higher CO tolerance compared to that of the untreated material.
- PtMo/C electrocatalysts suffer a partial dissolution of Mo during a 5000 times cycling aging.
- The stability of the PtMo/C electrocatalyst is improved after the 600 °C heating treatment.

ARTICLE INFO

Article history:
Received 20 July 2013
Received in revised form
29 August 2013
Accepted 31 August 2013
Available online 18 September 2013

Keywords:
PEMFC
CO tolerance
Stability
PtMo/C catalyst
Hydrogen oxidation

ABSTRACT

The effect of heat treatment on the activity, stability and CO tolerance of PtMo/C catalysts was studied, due to their applicability in the anode of proton exchange membrane fuel cells (PEMFCs). To this purpose, a carbon supported PtMo (60:40) alloy electrocatalyst was synthesized by the formic acid reduction method, and samples of this catalyst were heat-treated at various temperatures ranging between 400 and 700 °C. The samples were characterized by temperature programmed reduction (TPR), energy dispersive X-ray spectroscopy (EDS), X-ray diffraction (XRD), Transmission electron microscopy (TEM), X-ray absorption spectroscopy (XAS), cyclic voltammetry (CV), scanning electron microscopy (SEM) and wavelength dispersive X-ray spectroscopy (WDS). Cyclic voltammetry was used to study the stability, and polarization curves were used to investigate the performance of all materials as CO tolerant anode on a PEM single cell text fixture. The catalyst treated at 600 °C, for which the average crystallite size was 16.7 nm, showed the highest hydrogen oxidation activity in the presence of CO, giving an overpotential induced by CO contamination of 100 mV at 1 Acm^{-2}. This catalyst also showed a better stability up to 5000 potential cycles of cyclic voltammetry, as compared to the untreated catalyst. CV, SEM and WDS results indicated that a partial dissolution of Mo and its migration/diffusion from the anode to the cathode occurs during the single cell cycling. Polarization results showed that the catalytic activity and the stability can be improved by a heat treatment, in spite of a growth of the catalyst particles.

1. Introduction

Proton exchange membrane fuel cells (PEMFCs) have become promising power sources because of their low operating temperature, high power density and environment friendly characteristics [1]. Platinum, the most active electrocatalyst for hydrogen oxidation reaction, is unfortunately susceptible to CO poisoning even at a concentration as low as 10 ppm. Therefore, the effective implementation of PEMFCs depends on the development of anode electrocatalysts capable of tolerating impurities, especially CO, present in reformed hydrocarbon fuel streams.

The poisoning effect on Pt can be decreased by modifying the Pt particles by the addition of a second metal, either by the formation of an alloy or by promotion with a second metal oxide. Nowadays, much research is addressed to the PtRu alloy as anode electrocatalyst, because the PtRu alloy has a large CO tolerance and chemical stability among the catalysts developed so far [2–4]. However, due to the scarcity of Ru, there is a need to reduce the Ru

* Corresponding author.
E-mail address: edsont@iqsc.usp.br (E.A. Ticianelli).

0378-7753/$ – see front matter © 2013 Elsevier B.V. All rights reserved.
http://dx.doi.org/10.1016/j.jpowsour.2013.08.138

usage and develop catalysts without Ru species. Research done on alloys of Pt with a non-precious metal, such as Sn, Fe, Co, W or Mo, have found excellent CO tolerance of these materials when reformate gas is used [5–8]. Among all these bimetallic electrocatalysts, the PtMo alloys showed a most promising CO tolerance as compared to the state-of-art PtRu/C catalyst. Mukerjee et al. [9] reported that PtMo (4:1) catalyst exhibits a two-to-three fold enhancement in CO tolerance compared to PtRu (1:1). A wide range of bimetallic PtMo materials has been prepared and studied: single crystals of the true PtMo alloys [10], carbon supported PtMo catalyst and various Pt electrodes whose surface has been modified either with Mo oxides [10,11] or some other Mo species. PtMo/C has not been proved only to be an active electrocatalyst when reformate fuel stream is used, but it is also a strong candidate when the ethanol or methanol is used as fuel in PEMFCs. For ethanol oxidation, Anjos et al. [12] observed a shift toward less positive potential in the anodic sweep curve for PtMo when it was compared with pure Pt catalyst. Ordóñez et al. [13] reported an enhanced activity for methanol oxidation on Pt_4Mo_1/C catalyst, showing low onset potential (0.38 V versus RHE against 0.5 V versus RHE for Pt/C) and high current densities for the methanol oxidation reaction. The mechanism of CO tolerance of the PtMo catalysts has been extensively studied in the literature. Two mechanisms have been reported for the enhancement of CO tolerance of these materials: a conventional bifunctional mechanism, in which the adsorption of CO occurs on Pt sites and oxygen-containing species are generated on Mo sites [14–16], and an electronic effect that involves the weakening of the Pt–CO bond [16].

While a good CO tolerance of the anode electrocatalysts is a key challenge in fuel cell technology, a high level of catalyst stability is also required to tolerate the dynamic operating conditions involved in practical automotive applications. In particular variations in the voltage over load cycle may trigger a number of degradation processes, including carbon corrosion, Pt sintering and dissolution [17]. In the case of Pt-M alloys (where M = Mo or another metal), the acidic environment of the fuel cell may cause a partial loss of M from the alloy itself, possibly reducing catalytic activity. Therefore it is important to assess the degree of catalyst stability under conditions that simulate the real-life PEMFC anode operating conditions. Although carbon supported PtMo electrocatalysts have shown a CO tolerance up to threefold the tolerance of the state-of-the-art PtRu/C catalysts, their long term stability regarding the CO poisoning is under discussion. It has been shown that bimetallic PtMo/C electrocatalysts are inherently unstable and suffer from the gradual loss of Mo due to its dissolution [7,8].

One of the major approaches to improve electrocatalyst activity and stability is the thermal treatment [18]. Several heat treatment techniques such as traditional oven/furnace heating, microwave heat treatment, plasma thermal treatment and ultrasonic spray pyrolysis have been applied to prepare and treat PEM fuel cell electrocatalysts [19]. Among these, the traditional oven/furnace heating technique is the most widely used. In general it involves heating the catalyst under an inert (N_2, Ar, or He) or reducing (H_2) atmosphere, in the temperature range of 80–900 °C for 1–4 h.

In this work, carbon supported PtMo (60:40) catalysts, prepared by the formic acid reduction method, were heat-treated in the temperature range of 400–700 °C, by the traditional oven/furnace heating technique in the presence of reducing (H_2) atmosphere for 1 h. The purpose of the present study was to improve the activity and stability of PtMo/C catalysts, especially against load changes. A potential cycling protocol of cyclic voltammetry at a scan rate of 50 mV s^{-1} ranging from 0.1 to 0.7 V was applied to the anode to stimulate load changes during fuel cell operation. To evaluate the stability of the catalysts, the performances of membrane electrode assemblies (MEAs) were measured before and after potential cycles at the intervals of 1000 potential cycles and the polarization curves were compared.

2. Experimental

A PtMo/C (60:40 atomic proportion, 20 wt.% metal/C) catalyst was prepared by the formic acid reduction method [3–7,20] which consisted of simultaneous reduction of dihydrogen hexachloroplatinate hexahydrate ($H_2PtCl_6.6H_2O$, Aldrich) and tetrahydrate ammonium molybdate [$(NH_4)_6Mo_7O_{24}\cdot 4H_2O$, Mallinckrodt], using formic acid as reducing agent in the presence of carbon (Vulcan XC-72, Cabot). Pt supported on Vulcan XC-72 carbon with 20 wt.% metal/C was supplied by E-TEK. Temperature programmed reduction analysis of the catalyst samples were then performed by using a Micromeritics AutoChem II Chemisorption Analyzer. The reducing gas mixture used was 10% H_2/Ar. The H_2 consumption was measured by a thermal conductivity detector (TCD) and a liquid N_2/isopropanol bath was used to remove the moisture formed during hydrogen reduction. A catalyst sample of 16 mg in weight, a flow rate of reducing gas of 10 mL min^{-1} and a temperature ramp of 10 °C min^{-1} from 0 to 1000 °C were used. On the basis of the peaks obtained in the temperature programmed reduction (TPR) profile, the PtMo/C catalyst samples were then heat-treated under flowing H_2 atmosphere, at several temperatures, ranging from 400 to 700 °C for 1 h, with a ramping rate of 5 °C min^{-1}.

The Pt:Mo atomic ratio was determined by energy dispersive x-ray spectroscopy (EDS) in a scanning electron microscope LEO, 440 SEM-EDX system (Leica-Zeiss, DSM-960) with a microanalyser (Link analytical QX 2000) and a Si(Li) detector and using a 20 keV incident electron beam. Physical properties of the catalysts, such as crystallite/particle size distribution and lattice parameters, were determined by X-ray diffraction (XRD, RIGAKU model RU200B) in the 2θ range from 10 to 90° and using CuKα radiation and transmission electron microscopy (TEM, JOEL 3010 transmission electron microscope). TEM analyses were performed in the Brazilian Nanotechnology National Laboratory (LNNano), from the Centro Nacional de Pesquisa em Energia e Materiais (CNPEM), Campinas (SP) Brazil. The average crystallite sizes of the catalyst samples were determined by the Scherrer equation, using the Pt (220) peak of the diffraction patterns [21]. In order to compare the electronic properties of the Pt atoms before and after the electrochemical experiments, X-ray absorption spectroscopy (XAS) measurements were performed. The x-ray absorption near edge structure (XANES) of the Pt L_3 absorption edge was measured in the transmission mode, by using a homemade spectrochemical cell which enables to set virtually the same humidification, temperature and gas flux as in real fuel cells [3,28,29,35]. The working electrodes consisted of pellets formed by the dispersed catalyst materials agglutinated with Nafion and containing 6 mg Pt cm^{-2}. The Pt cathode fed with hydrogen was used as the reference electrode and the counter electrode was a Pt screen with a cut in the center in order to allow the free passage of the X-ray beam. These experiments were performed with the electrodes polarized at 50 mV vs. RHE. The XAS experiments were conducted at the XAS beamline of the Brazilian Synchrotron Light Laboratory.

Scanning electron microscopy (SEM) and electron probe microanalysis (EPMA) of cross sections of the MEAs (membrane electrode assemblies) were performed, in order to investigate the loss of Mo from the PtMo catalysts and its migration to the electrolyte membrane. To this purpose, samples of the new and cycled MEAs were cut transversely with scissors, then they were mounted on aluminum sample holder, and finally they were coated with a carbon layer, in order to increase their surface electrical and thermal conductivities. The SEM analysis was performed using a SIGMA (Carl Zeiss) field emission scanning electron microscope (FE-SEM),

and EPMA analysis was done with a JEOL JXA 8230 electron probe microanalyzer, using a wavelength dispersive spectrometer and a PETJ analyzer crystal. SEM and EPMA studies were carried out in the Laboratorio de Microscopía Electrónica y Análisis por Rayos X, from the Facultad de Matemática, Astronomía y Física (FAMAF), Universidad Nacional de Córdoba, Argentina.

The gas diffusion and catalyst layers of the electrodes for the PEMFC were prepared as described previously [3–6,8,22,23]. The gas diffusion layer was formed by applying a mixture of carbon powder (Vulcan XC-72, Cabot) with 15 wt. % of polytetrafluoroethylene (PTFE, TE 306A, Dupont) on to both sides of a carbon cloth substrate (PWB-3, Stackpole), using a loading (carbon + PTFE) of 3 mg cm^{-2} on each face. The catalyst layer was prepared from an homogeneous suspension formed by 0.1 mL of Nafion solution (Aldrich, 5 wt.%), the electrocatalysts (PtMo/C in the case of the anode and Pt/C in the case of the cathode) and 0.05 mL of isopropanol. The resulting mixture was homogenized in an ultrasonic bath for 10 min and was dried in air to obtain a solid material. This solid material was then mixed with isopropanol to produce an ink, which was then, applied by a brushing procedure on one face of each gas diffusion layer (of 4.62 cm^2 in area). The metal load was 0.4 mg cm^{-2} for both, anode (PtMo/C) and cathode (Pt/C, E-TEK). Membrane electrode assemblies (MEAs) were prepared by hot pressing the anode and cathode on both sides of a Nafion 115 membrane (Dupont) pre-treated at 125 °C and 5 MPa for 1 min. The MEAs were then placed between two high density graphite plates in which serpentine type gas distribution channels were machined. Fuel cell polarization measurements were carried out galvanostatically with a single cell at 85 °C, using oxygen saturated with Mili-Q water at 90 °C and 1.7 atm for the cathode, and either pure hydrogen or a mixture of hydrogen with 100 ppm CO saturated with Mili-Q water at 100 °C and 2 atm for the anode. Before the data acquisition, the system was first maintained at 0.7 V with pure H_2 for 2 h and then at 0.8 V with H_2/100 ppm CO, also for 2 h, to reach the steady state.

A cyclic voltammetry method was applied to the single cell electrodes to investigate the effect of potential cycling on the electrocatalyst stability, and its use as degradation testing technique [26,33]. The experiments were performed using a Solartron 1285 potentiostat/galvanostat in the standard fuel cell hardware. In these experiments the anode was used as the working electrode and cathode was used as the reference and counter electrodes. During the anode was exposed to argon and the cathode was exposed to hydrogen. The anode potential was cycled between 0.1 and 0.7 V, at a scan rate of 50 mV s^{-1}. The cycling was performed at room temperature, in increments of 1000 cycles up to a total of 5000 cycles. The performance of the MEAs was evaluated before and after each 1000 potential cycles, by measuring polarization curves and calculating anode overpotential due to the presence of CO (η_{CO}). This anode overpotential was calculated at each current density from the values of the cell potential in the absence (pure H_2) and presence (H_2 + 100 ppm CO) of CO [32,35]. Cyclic voltammetry was also applied to the cathode by the same procedure as for the anode, after the above-mentioned 5000 potential cycles.

3. Results and discussions

3.1. Characterization of PtMo/C electrocatalysts

Temperature programmed reduction technique was used to study the reducibility and reduction temperature of oxide species, such as platinum and molybdenum oxides, dispersed on the carbon support. Fig. 1 shows the TPR profile of the as-prepared PtMo/C catalyst, in which two hydrogen consumption peaks can be observed (at around 300 and 700 °C). The lower temperature

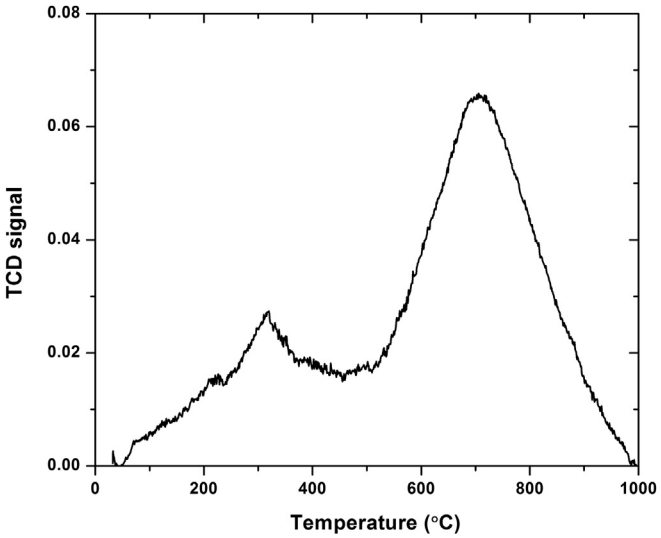

Fig. 1. TPR profile of the as-prepared PtMo/C catalyst carried out by passing a mixture of Ar/H_2 (10%) through a 16 mg sample with the designed temperature program: from 0 to 1000 °C at a heating rate of 10 °C min^{-1}.

reduction peak has normally been assigned to the reduction of MoO_3 [13,25],

$$2MoO_3 + 6H_2 \rightarrow 2Mo + 6H_2O \quad (1)$$

whereas the higher temperature reduction peak has usually been attributed to the reduction of MoO_2,

$$2MoO_2 + 4H_2 \rightarrow 2Mo + 4H_2O \quad (2)$$

Usually the reduction of these Mo species occurs at higher temperatures, but due to the presence of Pt, in this case the hydrogen consumption peaks for Mo species are shifted to lower temperatures. This is due to the fact that the hydrogen molecule is first activated and dissociated into H atoms on Pt centers at a low temperature, which then enter into the lattice of these Mo species, occupying interstitial sites and behaving as intermediate in the reduction of these species to lower the activation energy. Consequently the reduction temperature is substantially decreased in the presence of Pt. On the basis of these hydrogen consumption peaks the catalyst samples were then heat-treated under hydrogen atmosphere at various temperatures ranging from 400 to 700 °C during 1 h to reduce these surface Mo oxide species aiming to form a true alloy PtMo/C catalyst.

The composition of the PtMo/C catalyst samples was determined by EDS. The average concentration of Pt and Mo in the as-prepared and thermally treated catalysts resulted in Pt:Mo atomic ratios of 64:36 and 59:41, respectively. The structure and phase analyses of the catalyst samples were performed by XRD. The XRD patterns obtained are shown in Fig. 2. They have been recorded before and after heat treatments performed in the temperature range between 400 and 700 °C, and predominantly exhibit the peaks of the single-phase face-centered cubic (FCC) crystalline structure of Pt, corresponding to the (111), (200), (220), (311) and (222) planes [3]. The diffraction peak located around $2\theta = 25°$ corresponds to the (002) crystal plane of the hexagonal structure of the Vulcan XC-72R carbon support. Besides this peak, all patterns present only diffraction peaks associated to the Pt crystal structure, indicating the absence of any other segregated crystalline phase. No oxide phases have been detected, but they may be present in amorphous structures. The mean crystallite sizes were calculated

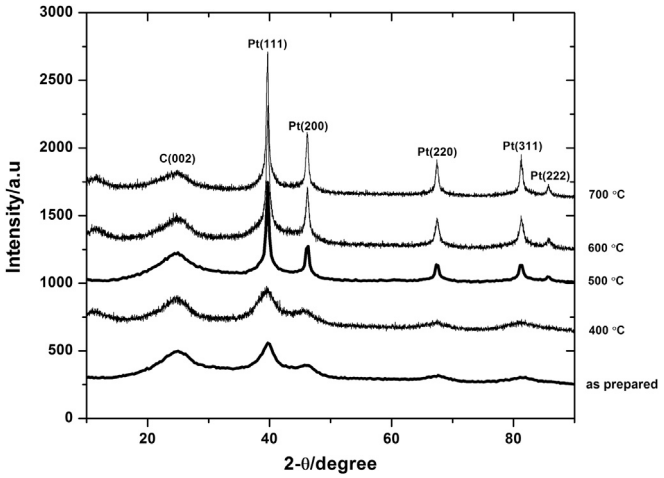

Fig. 2. XRD patterns of PtMo/C samples recorded before and after heat treatment at various temperatures.

from the (220) diffraction peak using the Scherrer equation. [34] The effect of the heat treatment on the crystallite size of the catalysts is shown in Fig. 3. As can be seen, the crystallite size of the catalyst increases as the heat treatment temperature increases, particularly above 500 °C. The crystallinity increased expectedly with the increasing temperature of heat treatment, as can be deduced from the sharpness and intensity of the diffraction peaks of the samples heat treated at different temperatures.

Fig. 4 shows typical TEM images of the as-prepared and heat-treated (600 °C) PtMo/C electrocatalysts, in which remarkably uniform and disperse alloy particles can be observed. Average particle diameters of 2.2 and 3.2 nm were determined from the TEM images, respectively. It is clear from the TEM image, that the crystallinity increases after the heat treatment, as also evidenced by XRD. Regarding the as-prepared catalyst, the average particle diameter is similar to the mean crystallite size determined from the corresponding XRD pattern by means of the Scherrer equation (see Fig. 3). This fact suggests that most of the particles are single crystals. In the case of the catalyst heat-treated at 600 °C, the

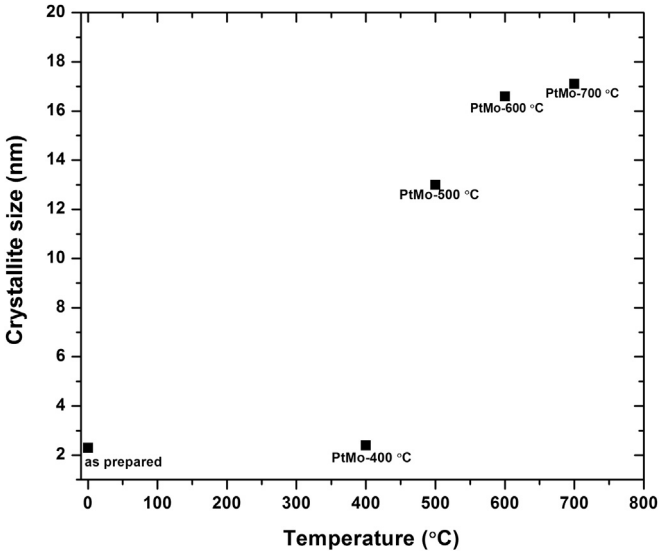

Fig. 3. Average crystallite size of the PtMo/C catalysts, before heat-treatment and after heat-treatment performed at various temperatures ranging from 400 to 700 °C.

average particle diameter (of 3.2 nm) obtained from the TEM images is noticeably lower than the mean crystallite size determined by XRD (around 15 nm, see Fig. 3). Clearly, these last two values are not consistent, because the particles cannot be smaller than the crystals. Doubtlessly, the size distribution of the group of particles analyzed by TEM does not represent the particle size distribution of the whole sample, and there must be bigger particles not recorded in the TEM images. It is worth mentioning that the particle size distributions were determined from sets of several TEM pictures. Then, for some reason, the big particles of the heat treated catalyst were not included in the sample holder for TEM analysis, perhaps due to some effect induced by the sample preparation. However, the behavior of the average crystallite size as a function of the temperature of the heat treatment (shown in Fig. 3) is very clear, and XRD results are more reliable than those of TEM, due to the larger statistic involved in the XRD analysis as compared with TEM.

To further investigate the effect of the heat treatment on the Pt 5d band properties in the PtMo/C electrocatalysts, XANES spectras were recorded at the Pt L_3 edge. Fig. 5 shows these spectra for both catalysts: the as-prepared PtMo/C and the heat-treated at 600 °C, polarized at 50 mV vs. RHE before and after CO adsorption. The X-ray absorption at the Pt L_3 edge corresponds to $2p_{3/2}$-5d electronic transitions and the magnitude of the hump (the so-called white line) located at about 5 eV is directly related to the occupancy of 5d electronic states [31]. The lower the occupancy, the higher the magnitude of the white line. A very small but consistent increase in the white line intensity is observed in the XANES spectra of the heat-treated PtMo/C electrocatalyst as compared with that corresponding to the as-prepared catalyst, in the presence of both H_2 (Fig. 5a) and H_2/CO (Fig. 5b) atmospheres. This indicates that the occupancy of the Pt 5d band in the PtMo/C catalysts increases marginally with the heat treatment. Some works showed that the number of Pt d band vacancies depends on the changes of particle size induced by heat treatments [39,40], as also seen in the present case. Santos et al. [24] demonstrated that for a PtV/C alloy electrocatalyst the occupancy of Pt 5d band practically remains the same when the temperature of heat treatment is increased from 300 to 850 °C. This was probably due to very small changes in particle size with the increase of heat treatment temperature. The effect of the particle size on the white line intensity of XANES spectra for Pt/C at various potential has been investigated previously [31]. A greater increase in the magnitude of white line with the increase in the applied potential is observed for the catalyst of small particle size (1 nm) in comparison to large particle sized (3.7 nm) catalyst. This increase in white line intensity with increasing applied potential for the catalysts with two different particle sizes is associated with a modification of average Pt oxidation state and has been discussed in detail by various authors [31,36,37]. Mukerjee et al. [9] observed a small increase in the Pt white line magnitude for PtMo/C when compared with Pt/C, indicating an increase in the number of Pt 5d band vacancies in PtMo/C due to alloying. A similar phenomenon is observed here, as seen from a comparison of the results in Fig. 5.

In order to study the effect of CO adsorption on the electronic properties of Pt, XANES spectra were also recorded for the Pt/C and PtMo/C catalysts before and after the CO adsorption, as shown in Fig. 5. In the case of Pt/C an increase in the white line intensity is clearly observed, when the catalyst is exposed to CO [32]. This is due to the fact that the adsorbed CO causes an increase in the number of Pt 5d band vacancies, compared to hydrogen alone, which is a result of the electron back-donation from Pt to CO. Similar but smaller effect is observed for the PtMo/C catalysts, as can be seen from comparison of the spectra shown in Fig. 5.

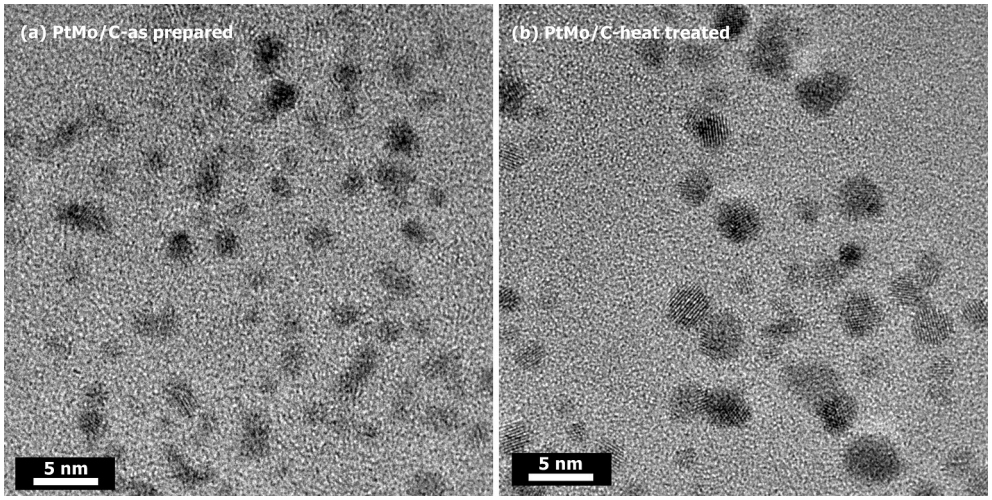

Fig. 4. TEM images and particle size distribution of as-prepared PtMo/C catalyst and the PtMo/C catalyst heat-treated at 600 °C.

3.2. Single cell performance of PtMo/C electrocatalysts

The performance and hydrogen oxidation activity of the PtMo/C electrocatalysts were evaluated by measuring the polarization curves both in the presence of pure H_2 and H_2 containing 100 ppm CO. Fig. 6 shows the single cell polarization curves obtained for anodes supplied with pure H_2 and H_2 containing 100 ppm CO for the as-prepared PtMo/C electrocatalyst and the catalysts heat-

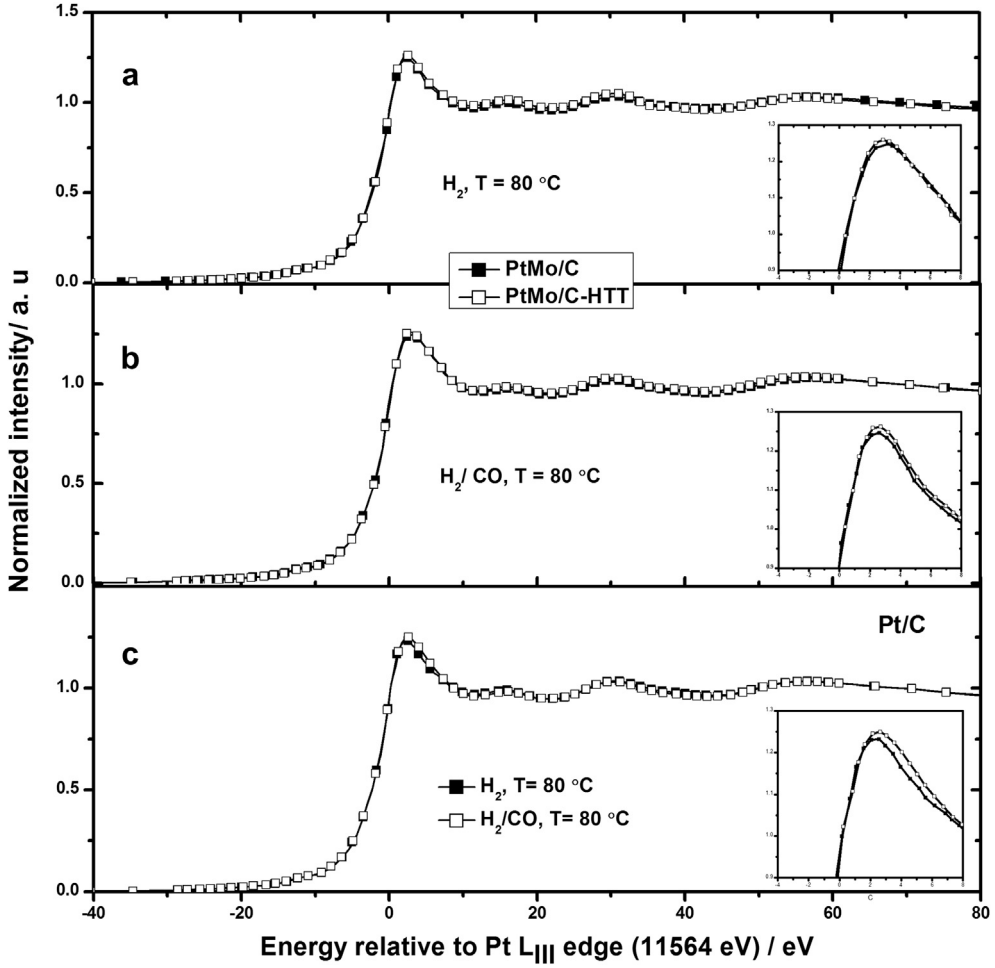

Fig. 5. XANES spectra of the Pt L_3 edge for the as-prepared PtMo/C catalyst (a and b), the PtMo/C catalyst heat-treated at 600 °C (a and b) and the commercial Pt/C catalyst (c); exposed to H_2 (a), H_2/CO (b) and both H_2 and H_2/CO (c).

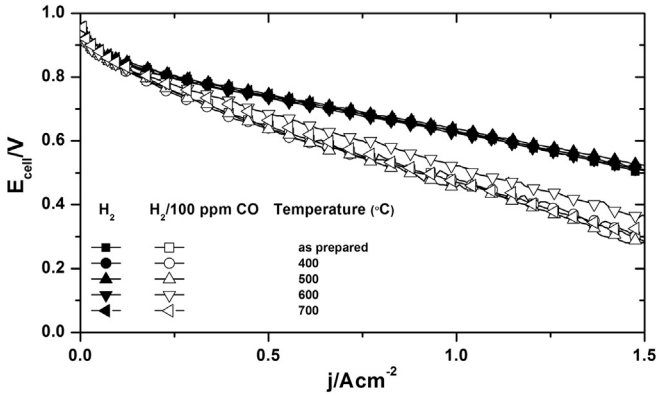

Fig. 6. PEM single cell polarization curves measured at 85 °C. The Pt/C cathodes were supplied with O_2; and the anodes (PtMo/C heat-treated at different temperatures) were supplied with pure H_2 and H_2/100 ppm CO.

treated at different temperatures, ranging from 400 to 700 °C. As can be seen, the PtMo/C electrocatalyst heat-treated at 600 °C, showed the highest hydrogen electro-oxidation activity in the presence of CO. This behavior may be related to the formation/stabilization of active Mo species for hydrogen oxidation in the presence of CO at 600 °C. Also, Han et al. [38] illustrated that the CO oxidation activity of Pt can be improved significantly by heat treatment and this enhances the hydrogen oxidation process. From here onward only the as-prepared PtMo/C catalyst and the heat-treated at 600 °C will be discussed. The polarization curves of these two catalysts, measured at several stages of the cycling process, supplied with both pure H_2 and H_2 containing 100 ppm CO are shown in Fig. 7. The corresponding anode overpotentials introduced by CO are shown in Fig. 8. The performance of the MEA was evaluated prior the cycling process and after each 1000 potential cycles, up to a total of 5000 cycles. As can be observed in Fig. 7, the performance declines significantly with the cycling process for the as-prepared catalyst (either if the anode is supplied with pure H_2 or with H_2 containing 100 ppm CO). In addition to this performance

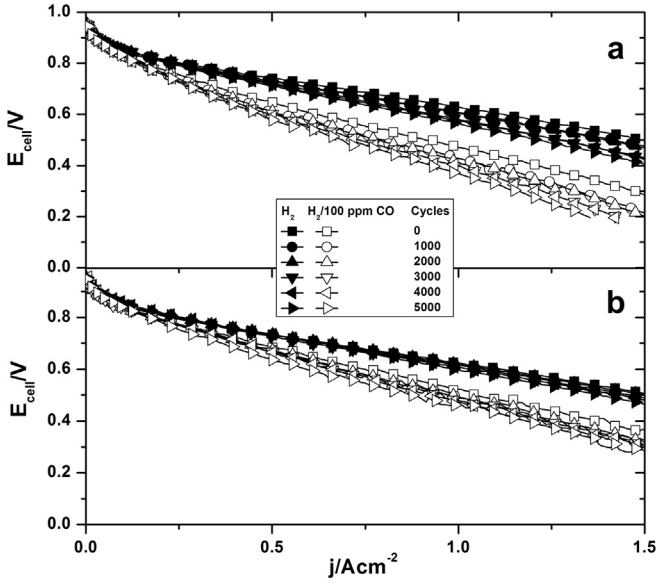

Fig. 7. PEM single cell polarization curves measured at 85 °C after multi-cycling treatments. The Pt/C cathodes were supplied with O_2; and the anodes (the as-prepared PtMo/C (a) and the heat-treated at 600 °C (b)) were supplied with pure H_2 and H_2/100 ppm CO.

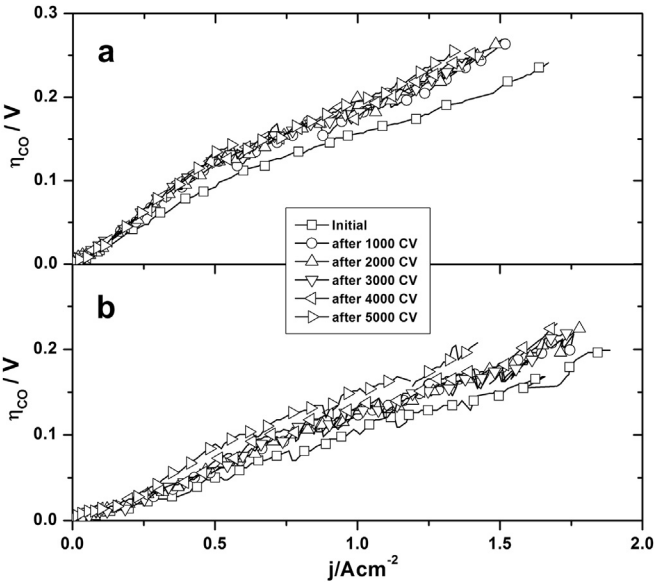

Fig. 8. Anode overpotential curves (η_{CO}) measured prior the cycling process and after each 1000 potential cycles, up to a total of 5000 cycles, for the untreated PtMo/C catalyst (a) and the PtMo/C catalyst heat-treated at 600 °C (b).

degradation, an increase of the anode overpotential due to the CO poisoning is also observed, as shown in Fig. 8a. However, the decline in the performance of the MEA prepared with the heat-treated catalyst is very small in both cases (with pure H_2, and with H_2 containing 100 ppm CO) even after 5000 cycles. Similarly, a small increase in anode overpotential was observed for this catalyst, as a result of the cycling process, as can be seen in Fig. 8b. A comparison between the anode overpotential of both catalysts after each 1000 cycles, for a current density of 1 Acm^{-2}, is shown in Fig. 9. A very little variation in the anode overpotential can be observed for the treated catalyst as compared to the as-prepared catalyst. These results show that the degradation of the cell performance could be effectively controlled by a heat treatment applied to the catalyst. Although the active surface area of the catalyst is reduced by a growth of the particles, induced by the heat treatment, this growth of the particles may have a positive effect on the catalyst stability, as the very fine particles are unstable [27,30].

3.3. Cyclic voltammetry and stability study of PtMo/C electrocatalysts

Cyclic voltammetry was performed to elucidate the surface properties of the electrocatalysts. The cyclic voltammograms of

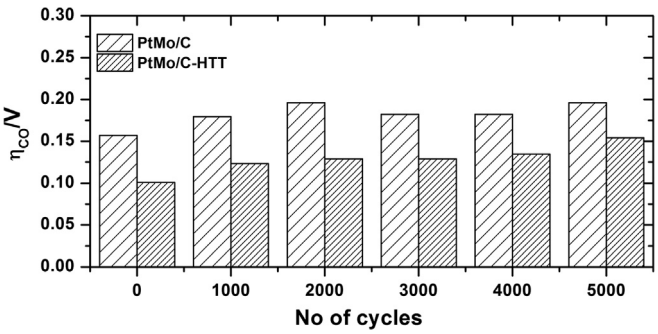

Fig. 9. Anode overpotential (η_{CO}) measured at 1 Acm^{-2} prior the cycling process and after each 1000 potential cycles, for the untreated catalyst and the catalyst heat-treated at 600 °C.

both, the as-prepared PtMo/C and treated electrocatalysts conducted in MEA arrangements are shown in Fig. 10. Besides the well-known hydrogen adsorption/desorption peaks located in the potential range of 0.15–0.35 V vs. RHE, a peak at about 0.45 V in the positive-going scan can be clearly seen for both electrocatalysts, while in the negative-going scan two weakly resolved peaks in the potential region between 0.2 V and 0.4 V vs. RHE can be observed. These peaks have generally been attributed to the reduction-oxidation of Mo, from Mo (IV) to Mo (VI) and vice versa. The present voltammetric results agree well with previously reported data [3,7,8,22,35].

The stability of both the as-prepared and the heat-treated PtMo/C catalysts was evaluated up to 5000 potential cycles, and the cyclic voltammograms shown in Fig. 10 are those recorded after each 1000 potential cycles.

A decrease in the current density was observed for both catalysts, as a consequence of the cycling process. However, for the as-prepared catalyst, the decrease in the current density is proportional to the number of cycles, whereas for the treated catalyst, the current density becomes practically constant after 2000 potential cycles.

This fact explains the small variation in the anode overpotential observed for the treated catalyst, in the polarization measurements. In both cases a decrease in the reduction-oxidation peaks of Mo is observed, which is an evidence that a dissolution of Mo from the anode takes place. This is confirmed by the cyclic voltammograms of the Pt/C cathode shown in Fig. 11, which were recorded after 5000 potential cycles of the anodes. The peak at 0.45 V, which is very characteristic of the presence of Mo species in the system, can be clearly observed. This shows that something of Mo is dissolved from the anode, and passes through the electrolyte membrane to reach the cathode, but eventually some Mo ionic species remain stuck in the electrolyte membrane.

In order to study the migration of these Mo species, scanning electron microscopy and x-ray analysis of both the new and cycled MEAs (with the as-prepared PtMo/C catalyst in the anode) were performed after the polarization measurements. Fig. 12a and b present scanning electron micrographs of cross sections of the MEAs, recorded with backscattered electrons, before the cycling process and after 5000 cycles, respectively. The carbon cloth, the

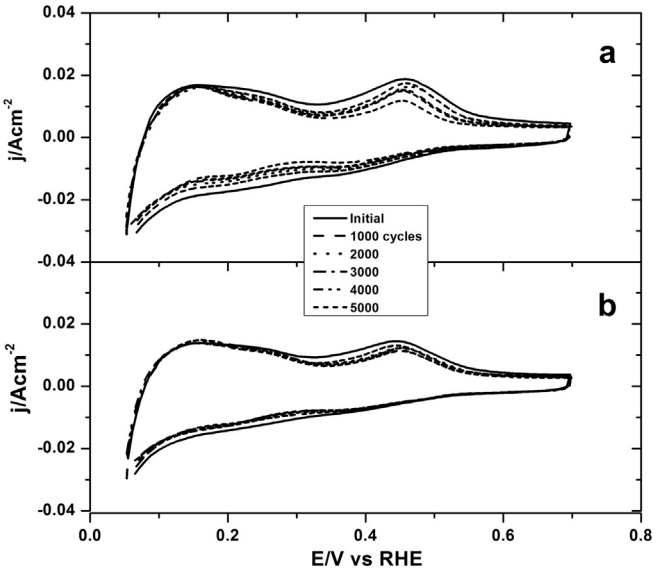

Fig. 10. Cyclic voltammograms of anodes composed of the untreated PtMo/C catalyst (a) and the PtMo/C catalyst heat-treated at 600 °C (b), after multiple cycles.

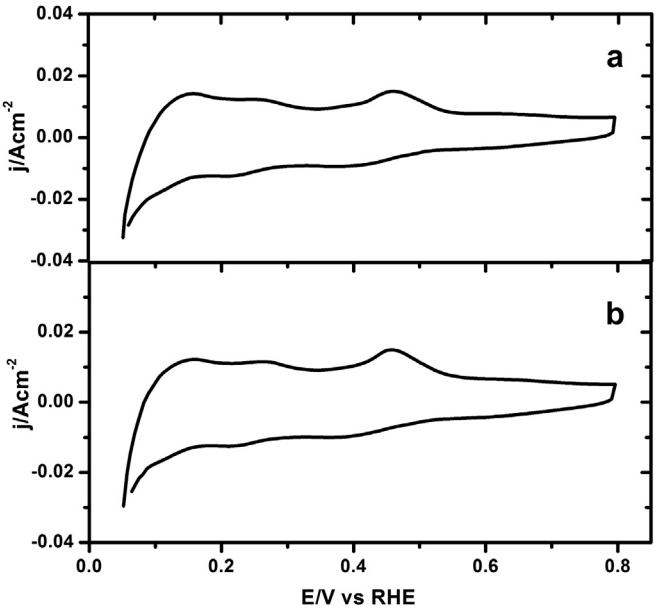

Fig. 11. Cyclic voltammograms of the Pt/C cathodes measured after 5000 potential cycles of the untreated PtMo/C anode (a) and the anode heat-treated at 600 °C (b).

anode and the cathode catalyst layers, and the membrane can be easily identified in the new and cycled MEAs. Some signs of deterioration can be appreciated in the cycled MEA, mainly related to structural and morphological features of their components.

Fig. 12c, d and e show x-ray spectra of the membrane, anode and cathode of both MEAs, recorded with a 20 keV incident electron beam and a wavelength dispersive spectrometer, in the energy range between 2.28 and 2.35 keV. These spectra were taken from the regions identified with white spots in Fig. 12a and b. As can be seen, the S-Kα peak is present in all the spectra, which is due to the sulfur content of the Nafion. The Mo-Lα peak and Pt-$M_3N_{4.5}$ peaks are also present in the spectra of the anodes, and Pt-$M_3N_{4.5}$ peak is present in the spectra of cathodes which correspond to metal content of PtMo and Pt/C catalysts, respectively. The presence of these peaks in the mentioned spectra is to be expected. However, the presence of Mo in the cathode of cycled MEA is also detected, as manifested by the Mo-Lα peak, indicated by an arrow in Fig. 12e. This fact is in agreement with the results of the cyclic voltammetry performed to the Pt/C cathodes after 5000 potential cycles (see Fig. 11). During cycling process, the Mo is partially dissolved from anode, passes through the membrane, and reaches the cathode, as was previously mentioned. On the other hand, a small amount of Pt can be appreciated in the membranes, as manifested by the Pt-$M_3N_{4.5}$ peak, indicated by an arrow in Fig. 12c, but in this case, the presence of Pt could be due to a contamination produced by the transversal cut of the MEAs during the sample preparation, because the presence of Pt is detected in both MEAs.

The significant decrease of the MEA performance indicates that the Mo species can interfere not only with the conduction of protons in the membrane, but also in the kinetics of oxygen reduction reaction (ORR) when they reach the cathode side.

There is scarce information in the literature about the stability of PtMo/C electrocatalysts. Lebedeva et al. [8] showed that PtMo/C catalysts prepared by formic acid and formaldehyde methods are unstable, and a gradual loss of Mo from the anode takes place due to its dissolution and its migration to the electrolyte. Long term stability measurements of PtMo/C catalysts under steady state condition at a cell voltage of 0.6 V were performed by Mukerjee et al. [9], which showed a very small variation in the performance

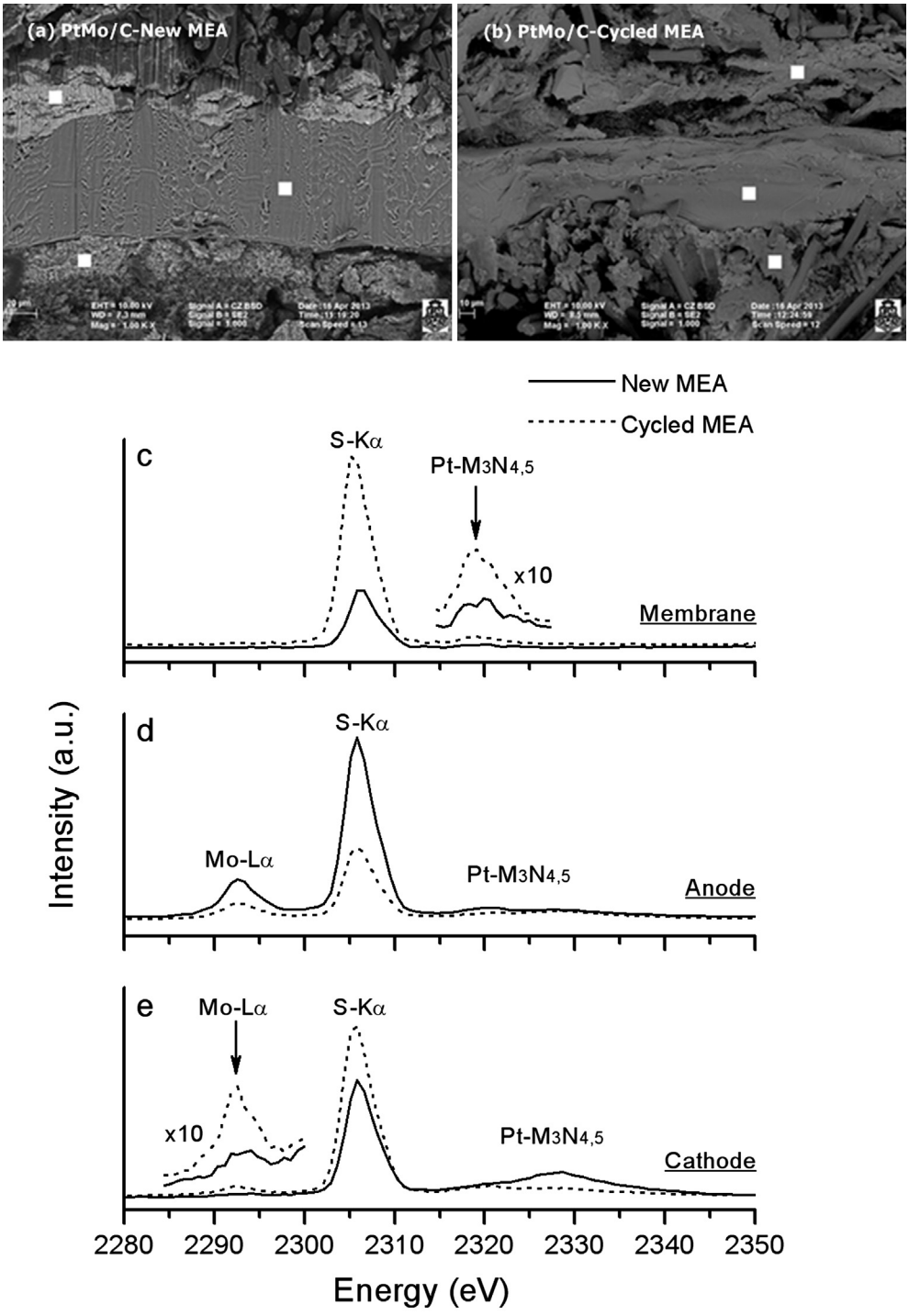

Fig. 12. Scanning electron micrographs of cross sections of the new (a) and cycled (b) MEAs, recorded with backscattered electrons. WDS spectra of the membranes (c), anodes (d) and cathodes (e) of both MEAs, acquired with a 20 keV incident electron beam, in the energy range between 2.28 and 2.35 keV, corresponding to the areas indicated with the white spots in the micrographs (a) and (b).

up to 1500 h of operation. However the Mo dissolution is one of the major cause of performance losses of these catalysts, which can be improved up to some extent by a heat treatment.

4. Conclusion

A carbon supported PtMo alloy electrocatalyst was synthesized by the formic acid reduction method. The effect of heat-treatment temperature on the catalyst electrocatalytic activity and stability was studied. The heat-treated catalyst showed an enhanced CO tolerance and a better stability as compared to the as-prepared catalyst, particularly due to the stabilization of the catalyst particle sizes at high temperature. Cyclic voltammetry measurements and WDS x-ray analysis showed that the PtMo/C alloy electrocatalysts suffered a partial dissolution of Mo during the cycling process, in which

something of Mo crossed the electrolyte membrane and reached the cathode.

Acknowledgment

The authors would like to thank the Third World Academy of Science (TWAS), Italy, the Conselho Nacional de Desenvolvimento Científico e Tecnológico (CNPq), the Brazilian Synchrotron Light Laboratory (LNLS), grant #2009/07629-6 from São Paulo Research Foundation (FAPESP), Brazil, and the Secretaría de Ciencia y Técnica (SeCyT) of the Universidad Nacional de Córdoba (UNC), Argentina, for financial supports.

References

[1] J. Kunze, U. Stimming, Angew. Chem. Int. Ed. 48 (2009) 9230.
[2] F. Hajbolouri, B. Andreaus, G.G. Scherer, A. Wokaun, Fuel Cells Fundam. Syst. 4 (2004) 160.
[3] H. Yu, Z. Hou, B. Yi, Z. LinH, J. Power Sources 105 (2002) 52.
[4] M. Watanabe, S. Motoo, J. Electroanal. Chem. 60 (1975) 267.
[5] L.G.S. Pereira, V.A. Paganin, E.A. Ticianelli, Electrochim. Acta 54 (2009) 1992.
[6] E.I. Santiago, V.A. Paganin, M. Carmo, E.R. Gonzalez, E.A. Ticianelli, J. Electroanal. Chem. 575 (2005) 53.
[7] G.A. Camara, M.J. Giz, V.A. Paganin, E.A. Ticianelli, J. Electroanal. Chem. 537 (2002) 21.
[8] N. P Lebedeva, G.J.M. Janseen, J. Electrochim. Acta 51 (2005) 29.
[9] S. Mukerjee, S.J. Lee, E.A. Ticianelli, J. McBreen, B.N. Grgur, N.M. Markovic, P.N. Ross, J.R. Giallombardo, E.S.D. Castro, Electrochem. Solid-State Lett. 2 (1999) 12.
[10] B.N. Grgur, G. Zhuang, N.M. Markovic, P.N. Ross, J. Phys. Chem. B 101 (1997) 3910.
[11] E.M. Crabb, M.K. Ravikumar, Y. Qian, A.E. Russell, S. Maniguet, J. Yao, D. Thompsett, M. Hurford, S.C. Ball, Electrochem. Solid-State Lett. 5 (2002) A5.
[12] D.M.D. Anjos, K.B. Kohohi, J.M.L. Geri, A.R.D. Andrade, P. Olivi, G.T. Filho, J. Appl. Electrochem. 36 (2006) 1391.
[13] L.C. Ordóñez, P. Roquero, P.J. Sebastian, J. Ramirez, Catal. Today 107 (2005) 46.
[14] P.P. Lopes, E.A. Ticianelli, J. Electroanal. Chem. 644 (2010) 110.
[15] F.J. Scott, S. Mukerjee, D.E. Ramaker, J. Electrochem. Soc. 154 (2007) A396.
[16] S.M.M. Ehteshami, S.H. Chan, Electrochim. Acta 93 (2013) 334.
[17] R.L. Borup, J.R. Davey, F.H. Garzon, D.L. Wood, M.A. Inbody, J. Power Sources 163 (2006) 76.
[18] A.N. Valisi, T. Maiyalagan, L. Khotseng, V. Linkov, S. Pasupathi, Electrocatalysis 3 (2012) 108.
[19] C.W.B. Bezerra, L. Zhang, H. Liu, K. Lee, A.L.B. Marques, E.P. Marques, H. Wang, J. Zhang, J. Power Sources 173 (2007) 891.
[20] V.A. Paganin, T.J.P. Freire, E.A. Ticianelli, E.R. Gonzalez, Rev. Sci. Instrum. 68 (1997) 3540.
[21] V. Radmilovic, H.A. Gasteiger, P.N. Rose, J. Catal. 154 (1995) 98.
[22] S. Mukerjee, R.C. Urian, S.J. Lee, E.A. Ticianelli, J. McBreen, J. Electrochem. Soc. 151 (2004) A1094.
[23] E.I. Santiago, M.S. Batista, E.M. Assaf, E.A. Ticianelli, J. Electrochem. Soc. 151 (2004) A944.
[24] L.G.R.A. Santos, K.S. Freitas, E.A. Ticianelli, Electrochim. Acta 54 (2009) 5246.
[25] K. Matsutani, K. Hayakawa, T. Tada, Platinum Metals Rev. 54 (2010) 223.
[26] P. Arnoldy, J.C.M. Jonge, J.A.M. Igarashi, T. Fujino, Y. Zhu, H. Uchida, M. Watanabe, J. Phys. Chem. 89 (1985) 4517–4526.
[27] S. Ball, A. Hodgkinson, G. Hoogers, S. Maniguet, D. Thompsett, B. Wong, Electrochem. Solid-State Lett. 5 (2002) A31.
[28] L.G.S. Pereira, F.R. Santos, M.E. Pereira, V.A. Paganin, E.A. Ticianelli, Electrochim. Acta 51 (2006) 4061.
[29] A.C. Garcia, V.A. Paganin, E.A. Ticianelli, Electrochim. Acta 53 (2008) 4309.
[30] S. Horn, Y.P.J. Ferreira, G.J. la O', D.D. Morgan, H.A. Gasteiger, R. Makharia, Electrochem. Trans. 1 (2006) 185.
[31] A.E. Russell, A. Rose, Chem. Rev. 104 (2004) 4613.
[32] T.C.M. Nepel, P.P. Lopes, V.A. Paganin, E.A. Ticianelli, Electrochim. Acta 88 (2013) 217.
[33] R. Borup, J.R. Davey, F.H. Garzon, D.L. Wood, M.A. Inbody, J. Power Sources 163 (2006) 76.
[34] J.R.C. Salgado, E.R. Gonzalez, Electrica Quimica 2 (2003) 77.
[35] E.I. Santiago, G.A. Camara, E.A. Ticianelli, Electrochim. Acta 48 (2003) 3527.
[36] A. Witkowska, E. Principi, A.D. Cicco, S. Dsoke, R. Marassi, L. Olivi, M. Centazzo, V.R. Albertini, J. Non-Cryst. Solids 354 (2008) 4227.
[37] E. Principi, A. Witkowska, S. Dsoke, R. Marassic, A.D. Cicco, Phys. Chem. Chem. Phys. 11 (2009) 9987.
[38] K.S. Han, Y.S. Moon, O.H. Han, K.J. Hwang, I. Kim, H. Kim, Electrochem. Commun. 9 (2007) 317.
[39] E. Antolini, J.R.C. Salgado, M.J. Giz, E.R. Gonzalez, Int. J. Hydrogen Energy 30 (2005) 1213.
[40] M. Min, J. Cho, K. Cho, H. Kim, Electrochim. Acta 45 (2000) 4211.